A Quantum Chemical View on the Mechanism of the Ta^+-Mediated Coupling of Carbon Dioxide with Methane

Nadja Sändig and Wolfram Koch*

Institut für Organische Chemie, Technische Universität Berlin, Strasse des 17. Juni 135, D-10623 Berlin, Germany

Received December 31, 1997

The mechanistic details of the coupling of methane and carbon dioxide mediated by a bare tantalum cation observed experimentally in the gas phase have been unraveled by means of quantum chemical calculations employing approximate density functional theory. All relevant intermediates and saddle points along the reaction coordinate have been located on the singlet and triplet potential energy surfaces. The energetically most favorable path has been identified and is characterized by several changes of the spin multiplicity. The reaction mechanism predicted by our calculations is in harmony with the available experimental information but provides additional information into the various elementary steps of this reaction, which could not be obtained by experimental means.

Introduction

The public interest in carbon dioxide grows steadily, mainly because of the increased influx of CO_2 in the atmosphere due to industrialization, which is suspected to contribute to the global greenhouse effect. From a more chemical point of view, the role of CO_2 as a potential C1 building block in chemical transformations is another important aspect of the chemistry of this simple and ubiquitous molecule. That carbon dioxide indeed can be used for this purpose is amply demonstrated by nature in many enzymatic processes. Thus, this theme represents a fascinating scientific challenge for experimental and theoretical chemists.[1] The past few years have witnessed significant advances in understanding the organometallic chemistry and the mechanistic details of biochemical processes which involve reactions of CO_2.[2] Among the chief targets of carbon dioxide chemistry is the efficient, simultaneous coupling of CO_2 with alkanes RH to yield the corresponding carbonic acids RCO_2H. Unfortunately, even from an energetic point of view the route to this reaction is paved with obstacles: the formation of acetic acid from CO_2 and CH_4 is endergonic under standard conditions and is even 9 kcal mol^{-1} endothermic in the gas phase.[3] Among the most prominent strategies of how such energetic hurdles can be overcome is complexation of the reactants and products to a metal center.[1] In recent years many reactions involving transition metals have been investigated experimentally in the gas phase, mainly by mass spectrometric methods. Thus, any interfering effects of ligating groups are avoided and the intrinsic properties of the metal ions can be unraveled.[4] Since experiments alone are usually not sufficient to completely deduce a whole reaction sequence, including energetic and structural information about all relevant saddle points and intermediates, parallel computational studies have proven to be of utmost importance for completing this ambitious task. Approximate density functional theory (DFT) has evolved as a particularly successful quantum chemical approach for studying reaction mechanisms involving open-shell transition-metal compounds. A number of recent studies have convincingly demonstrated that DFT, in particular with Hartree−Fock/DFT hybrid functionals such as Becke3LYP, affords at least qualitatively correct results at moderate computational costs, even for describing complicated electronic structures common in open-shell transition-metal chemistry.[5]

The current investigation was triggered by a recent experimental study by Wesendrup and Schwarz.[6] These authors were investigating the possibility of using a transition-metal ion to couple carbon dioxide with methane by generating a C−C bond between these two entities. While the cations Ta^+, W^+, Os^+, Ir^+, and Pt^+ of the third transition-metal row react exothermically with methane, forming the respective carbene complex MCH_2^+ and molecular hydrogen,[7] only the metal−oxygen bonds M^+−O of Ta^+ and W^+ are strong enough to reduce carbon dioxide exothermically. With both cations the monoxide MO^+ is generated in a first step

(1) Behr, A. *Carbon Dioxide Activation by Metal Complexes*; VCH: Weinheim, Germany, 1988. Ayers, W. M., Ed. *Catalytic Activation of Carbon Dioxide*; ACS Symposium Series 363; American Chemical Society: Washington, DC, 1988. Aresta, M., Schloss, J. V., Eds. *Enzymatic and Model Carboxylation and Reduction Reactions for Carbon Dioxide Utilization*; NATO ASI Ser. Ser. C; Kluwer Academic: Dordrecht, The Netherlands, 1990.

(2) Walther, D. *Nachr. Chem.-Technol. Lab.* **1992**, *40*, 1214. Kitajima, N.; Hikichi, S.; Tanaka, M.; Moro-oka, Y. *J. Am. Chem. Soc.* **1993**, *115*, 5496. Leitner, W. *Angew. Chem.* **1994**, *106*, 183. Willner, I.; Willner, B. *Top. Curr. Chem.* **1991**, *159*, 153.

(3) Lias, G.; Bartmess, J. E.; Liebman, J. F.; Holmes, J. L.; Levin, R. D.; Mallard, W. G. Gas-Phase Ion and Neutral Thermochemistry. *J. Phys. Chem. Ref. Data. Suppl. 1* **1988**. Lias, G.; Liebman, J. F.; Levin, R. D.; Kafafi, S. A. *NIST Standard Reference Database, Positive Ion Energetics*, Version 2.01; NIST: Gaithersburg, MD, 1994.

(4) See, e.g.: Armentrout, P. B. *Annu. Rev. Phys. Chem.* **1990**, *41*, 313. Eller, K.; Schwarz, H. *Chem. Rev.* **1991**, *91*, 1121. Freiser, B. S. *Acc. Chem. Res.* **1994**, *27*, 353.

(5) See, e.g., Bauschlicher, C. W. Jr.; Ricca, A.; Partridge, H.; Langhoff, S. R. in *Recent Advances in Density Functional Methods, Part II*, Chong, D. P. (ed.), World Scientific: Singapore, 1997; Koch, W.; Hertwig, R. H. in *The Encyclopedia of Computational Chemistry*, Schleyer, P. v. R. (ed.), Wiley: New York, in press.

(6) Wesendrup, R.; Schwarz, H. *Angew. Chem.* **1995**, *107*, 2176.

S0276-7333(97)01141-2 CCC: $15.00
Publication on Web 05/08/1998

and subsequently the dioxide MO_2^+ is formed. The formation of a C−C bond is, however, thermodynamically only possible by using Ta^+. The overall reaction sequence is shown in Scheme 1 and will be discussed in more detail in a subsequent section. Briefly, it consists of three individual steps: in the first one, tantalum carbene is formed, which in a second step reacts with a carbon dioxide molecule to generate a Ta(O)CH_2^+ species. Finally, this intermediate reacts with a second CO_2 to yield C_2H_2O with release of TaO_2^+.

Scheme 1

$$Ta^+ + CH_4 \rightarrow TaCH_2^+ + H_2 \qquad \text{(I)}$$

$$TaCH_2^+ + CO_2 \rightarrow Ta(O)CH_2^+ + CO \qquad \text{(II)}$$

$$Ta(O)CH_2^+ + CO_2 \rightarrow TaO_2^+ + C_2H_2O \qquad \text{(III)}$$

$$Ta^+ + CH_4 + 2CO_2 \rightarrow TaO_2^+ + H_2 + CO + C_2H_2O$$

The detailed reaction mechanisms of the elementary steps of this reaction are not yet known and call for a comprehensive theoretical investigation. The following study concentrates on the second and third parts of this sequence, i.e., those where the carbon dioxide is actually involved in the process. The first step, i.e., the activation of a C−H bond in methane brought about by a tantalum cation, yielding $TaCH_2^+$ and molecular hydrogen, was already described using a very similar computational approach in an earlier investigation in this journal.[8] Together with these previous results, we will provide a complete and consistent picture of the tantalum-cation-mediated C−C coupling reaction between methane and CO_2.

Methods

A detailed discussion of the theoretical strategy and a careful calibration of the level of accuracy has already been given in ref 8. Therefore, we restrict ourselves to a brief summary of the computational procedures at this point. We used the Becke3LYP hybrid functional (B3LYP)[9] as implemented in Gaussian 94.[10,11] This functional has repeatedly been shown to be the most reliable one in modern DFT, in particular for applications in transition-metal chemistry.[5] The 60 *core* electrons ([Kr], $4d^{10}$, $4f^{14}$) of the tantalum cation were described by the relativistic effective core potential (RECP) of Dolg et al.[12] This RECP was combined with a valence basis for the remaining tantalum electrons of (8s7p6d) → (6s5p3d)/[311111|22111|411] quality. Oxygen, carbon, and hydrogen were described by Dunning's standard split-valence D95 basis set.[13] Using this basis set, hereafter designated as BS1, all geometries were optimized using analytical gradient procedures. The analytically calculated force constant matrixes were evaluated for the characterization of the stationary points (minima or transition states) and the determination of zero point vibrational energies (ZPVE) and thermal corrections. On several occasions it was necessary to reduce the actual point group symmetry to slightly symmetry broken C_1-symmetric structures, since unexpected negative eigenvalues for minima appeared.[14] All structures reported correspond to fully converged geometries with gradients as well as displacements below the standard thresholds implemented in Gaussian 94.

Table 1. Theoretical Thermochemistry (in kcal mol⁻¹) for the Reaction $Ta^+ + 2CO_2 + CH_4 \rightarrow TaO_2$ ($^1A_1$) + $C_2H_2O^+ + H_2$

ΔH(0 K)	−49.9
ΔH(0 K) + ZPVE	−50.5
ΔH(298 K)	−55.9
$T\Delta S$(298 K)	+4.6
ΔG(298 K)	−60.5

For obtaining more reliable relative stabilities, single-point energy calculations were performed with a more flexible one-particle description: the Ta^+ basis set was augmented by one *f* function ($\alpha_f = 0.790$), and the polarized 6-31G(d,p) basis set was employed for the oxygen, carbon, and hydrogen atoms.[15] In the following, this RECP/basis combination will be designated as BS2.

All relative energies are corrected for ZPVE, entropic and thermal contributions and correspond to free enthalpies at 298 K, ΔG^{298}. Thus, the calculated results are directly comparable to the experimental data. To provide an idea of the magnitudes of the various corrections, they are explicitly listed for the energetics of the overall reaction $Ta^+ + 2CO_2 + CH_4 \rightarrow TaO_2^+ + H_2 + CO + C_2H_2O$ in Table 1. Thus, in terms of total energies alone, the products are more stable than the reactants by 49.9 kcal mol^{-1}. After inclusion of the differences in ZPVE, a theoretically predicted reaction exothermicity ($\Delta H_R° = \Delta U_R°$) of −50.5 kcal mol^{-1} is obtained for 0 K. At 298 K the exothermicity (ΔH_R^{298}) changes by some 5 kcal mol^{-1} to −55.9 kcal mol^{-1}. If we take into account also the entropy difference of +4.6 kcal mol^{-1} between $Ta^+/CH_4/2CO_2$ and $TaO_2^+/C_2H_2O/H_2$, the final value for the Gibbs energy, ΔG_R^{298}, of this reaction amounts to −60.5 kcal mol^{-1} at 298 K. For comparison, from literature thermochemical data,[3] Wesendrup and Schwarz[6] report an overall exothermicity (ΔH_R) of 53 kcal mol^{-1}, only 3 kcal mol^{-1} off the theoretically predicted number.

Due to the lack of frequencies at the BS2 level, the corrections obtained from the BS1 frequencies were used throughout. All bond lengths and angles are specified in angstroms (Å) and in degrees (deg). While spin-free, kinematic relativistic effects are covered through the RECP, no corrections for spin−orbit coupling have been included. Since for an element as heavy as Ta spin−orbit coupling is not negligible (for example, the experimental $^5F_1$ ground state of the Ta^+ ion is 3755 cm^{-1} or 10.7 kcal mol^{-1} lower in energy than the *J*-averaged ^5F term[16]), neglecting these effects does obviously introduce a certain error margin in our computed data. It is probably safe to assume that the spin−orbit stabilization of some 11 kcal mol^{-1} in the Ta^+ atom provides an upper bound to the spin−orbit stabilization in any Ta^+-containing compound, because the electron distribution in a molecule is much

(7) Irikura, K. K.; Beauchamp, J. L. *J. Am. Chem. Soc.* **1989**, *111*, 75; Buckner, S. W.; MacMahon, T. J.; Byrd, G. L.; Freiser, B. S. *Inorg. Chem.* **1989**, *28*, 3511; Irikura, K. K.; Beauchamp, J. L. *J. Am. Chem. Soc.* **1991**, *113*, 2796; Heinemann, C.; Wesendrup, R.; Schwarz, H. *Chem. Phys. Lett.* **1995**, *239*, 75.
(8) Sändig, N.; Koch, W. *Organometallics* **1997**, *16*, 5244.
(9) Becke, A. D.; *J. Chem. Phys.*, **1993**, *98*, 5648; *ibid.* **1993**, *98*, 1372.
(10) Stephens, P. J.; Devlin, F. J.; Chabalowski, C. F.; Frisch, M. J. *J. Phys. Chem.* **1994**, *98*, 11623.
(11) Frisch, M. J.; Trucks, G. W.; Schlegel, H. B.; Gill, P. M. W.; Johnson, B. G.; Robb, M. A.; Cheeseman, J. R.; Keith, T.; Peterson, G. A.; Montgomery, J. A.; Raghavachari, K.; Al-Laham, M. A.; Zakrzewski, V. G.; Ortiz, J. V.; Foresman, J. B.; Peng, C. Y.; Ayala, P. Y.; Chen, W.; Wong, M. W.; Andres, J. L.; Replogle, E. S.; Gomperts, R.; Martin, R. L.; Fox, D. J.; Binkley, J. S.; DeFrees, D. J.; Baker, J.; Stewart, J. P.; Head-Gordon, M.; Gonzalez, C.; Pople, J. A. Gaussian 94, Revision B.3; Gaussian, Inc.: Pittsburgh, PA, 1995.
(12) Dolg, M.; Wedig, U.; Stoll, H.; Preuss, H. *J. Chem. Phys.* **1987**, *86*, 866.
(13) Dunning, T. H., Jr.; Hay, P. J. in *Modern Theoretical Chemistry*; Schaefer, H. F., III, Ed.; Plenum: New York, 1976; pp 1−28.
(14) Such effects have been noted before. See, e.g.: Holthausen, M. C.; Fiedler, A.; Schwarz, H.; Koch, W. *J. Phys. Chem.* **1996**, *100*, 6236.
(15) Frisch, M. J.; Pople, J. A.; Binkley, J. S. *J. Chem. Phys.* **1984**, *80*, 3265.
(16) Moore, C. E. *Atomic Energy Levels*; NSRDS-NBS Circular No. 467; US GPO: Washington, DC, 1949.

more delocalized than in the atom and there will be considerable quenching of the spin−orbit stabilization. Because the atomic ion will benefit much more from the spin−orbit stabilization than will the molecule, the most obvious effect of the neglect of any spin−orbit interaction will be an overestimation of binding energies, in particular if the bare Ta^+ ion is involved. Furthermore, since the different states of a particular species will not profit equally from spin−orbit interactions, there will also be an impact on the relative energetics of the various multiplicities discussed below. The stabilization will be smallest for states with $S = 0$ and will probably increase with the number of unpaired electrons. However, this differential stabilization will certainly be significantly smaller than the effect on the binding energies. An estimate on the quantitative role of spin−orbit effects can be extracted from an explicit four-component Dirac−Fock MP2 treatment of the closely related $PtCH_2^+$ molecule. Here, the spin−orbit stabilization in the molecule was about half as large as in the Pt^+ ion.[17] If in the present case a similar quenching occurs, the uncertainty in our computed binding energies produced by the neglect of spin−orbit effects should be on the order of 5 kcal mol^{-1} and will certainly not exceed 10−11 kcal mol^{-1}. The error for the relative stabilities of different spin states will be much smaller. Also, the effects of the basis set superposition error are expected to be of minor importance; its order of magnitude has been documented in ref 8 as amounting to a few kilocalories per mole. However, we do not simply correct the interaction energies by this amount, since it is well-known that the BSSE is always interwoven with the error induced by the incompleteness of the one-particle description. The latter effect will lower the binding energy, and to a certain (but usually unknown) extent, these two effects cancel.[18−20] Overall, we expect our energetic data to be accurate within a few kilocalories per mole.[8]

In the following, all energetic data will refer to the B3LYP/BS2 results with ZPVE, thermal corrections, and entropic contributions obtained at the B3LYP/BS1 level of approximation. The calculations were performed with Gaussian 94 installed on our own IBM RS/6000 workstations as well as on CRAY-J90 computers at the Konrad-Zuse Zentrum für Informationtechnik, Berlin.

Experimental Background

As indicated in the Introduction, the gas-phase reaction $Ta^+ + CH_4 + 2CO_2 \rightarrow TaO_2^+ C_2H_2O + CO + H_2$ was recently investigated in detail by Wesendrup and Schwarz using Fourier transform-ion cyclotron resonance mass spectrometry.[6] We will briefly summarize their main conclusions relevant in the present context.

The desired C−C coupling does not take place if the initial step consists of the reaction between Ta^+ and CO_2 to form an oxygenated tantalum species, which in a subsequent step should undergo a reaction with methane. TaO^+ is the primary ionic product of this reaction of Ta^+ and CO_2, which reacts further to the dioxide, TaO_2^+, as the final ionic product. Both reactions are strongly exothermic (experimental: −57 and −29 kcal mol^{-1},[6] respectively; we compute −51.0 and −30.9 kcal mol^{-1}, respectively, supporting the level of confidence we assign to our calculations). However, in contrast to the late transition metals,[4] these cationic tantalum oxides do not react with methane; rather, they represent a dead end in this process. Thus, the reaction sequence was changed and commences with the formation of the carbene complex $TaCH_2^+$ as an activated methane equivalent, from Ta^+ and CH_4. This carbene complex reacts rapidly in the second part of the reaction sequence with CO_2. During this process CO_2 is reduced to CO and a $[Ta,C,H_2,O]^+$ species is generated. The authors suggested five possible structures, **a**−**e**, for this complex (see Chart 1).[6] On account of thermochemical considerations, formation of the Ta^+−formaldehyde complex **d** could be excluded: the reaction leading to this complex could only occur if the binding energy between the formaldehyde ligand and the metal amounts to at least 70 kcal mol^{-1}, which is certainly not the case. The CO/H_2 complex **e** is discounted for similar reasons. On the basis of the assumption that the Ta^+−C bond of the tantalum carbene complex is not broken in the $[Ta,C,H_2,O]^+$ species and that the oxygen is connected to the metal, species **a**−**c** are reasonable. Since no loss of an OH radical was observed in the mass spectra, the hydroxy−carbene complex **b** drops out as a likely candidate for the $[Ta,C,H_2,O]^+$ species. Thus, only the oxo−carbene complex **a** and the oxametallacycle **c** are consistent with the experimental data. An unequivocal distinction between these two was, however, impossible based solely on the mass spectrometric information.[6]

Chart 1. Structures Proposed for the [Ta, C, H_2, O]$^+$ Species

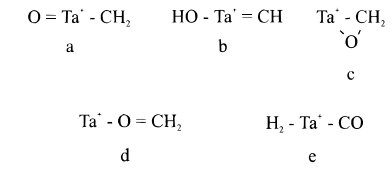

Most interestingly, regardless of its actual connectivity, the $[Ta,C,H_2,O]^+$ species undergoes a further, albeit slow, reaction with a second equivalent of CO_2, yielding tantalum dioxide, TaO_2^+, as the sole ionic product. Again, the experimental data were insufficient for an identification of the nature of the neutral product, $[C_2,H_2,O]$. Nevertheless, the number of possible structural isomers can be reduced by using the known heats of formation of possible $[C_2,H_2,O]$ isomers.[21] The overall reaction $Ta^+ + CH_4 + 2CO_2 \rightarrow TaO_2^+ + C_2H_2O + CO + H_2$ can only be exothermic if the neutral product is ketene ($\Delta H_r = -53$ kcal mol^{-1}) or, albeit to a significantly lesser extent, hydroxyacetylene ($\Delta H_r = -16$ kcal mol^{-1}). On mechanistic grounds, the formation of a HC≡COH molecule from either **a** or **c** would seem to be very difficult. On the other hand, a metathesis reaction involving **a** and CO_2 thereby effectively linking the two C_1 building blocks CO_2 and CH_4 to ketene appears plausible and is favored by Wesendrup and Schwarz.[6] Interestingly, Proloux and Bergman reported recently a comparable reaction in the condensed phase, where a tantalum carbene complex reacted with a CO

(17) Heinemann, C.; Schwarz, H.; Koch, W.; Dyall, K. G. *J. Chem. Phys.* **1996**, *104*, 4642.
(18) Taylor P. R. In *Lecture Notes in Quantum Chemistry*; Roos, B. O., ed.; Springer: Berlin, 1992.
(19) Frenking, G.; Antes, I.; Böhme, M.; Dapprich, S.; Ehlers, A. W.; Jonas, V.; Neuhaus, A.; Otto, M.; Stegmann, R.; Veldkamp, A.; Vyboishikov, S. F. In *Reviews in Computational Chemistry*; Lipkowitz, K. B., Boyd, D. B., Eds.; VCH: New York, 1996; Vol. 8.
(20) Dargel, T. K.; Hertwig, R. H.; Koch, W.; Horn, H. *J. Chem. Phys.* **1998**, *108*, 3876.
(21) Baar, B. van Weiske, T.; Terlouw, H.; Schwarz, H. *Angew. Chem.* **1986**, *98*, 275; *Angew. Chem., Int. Ed. Engl.* **1986**, *25*, 282.

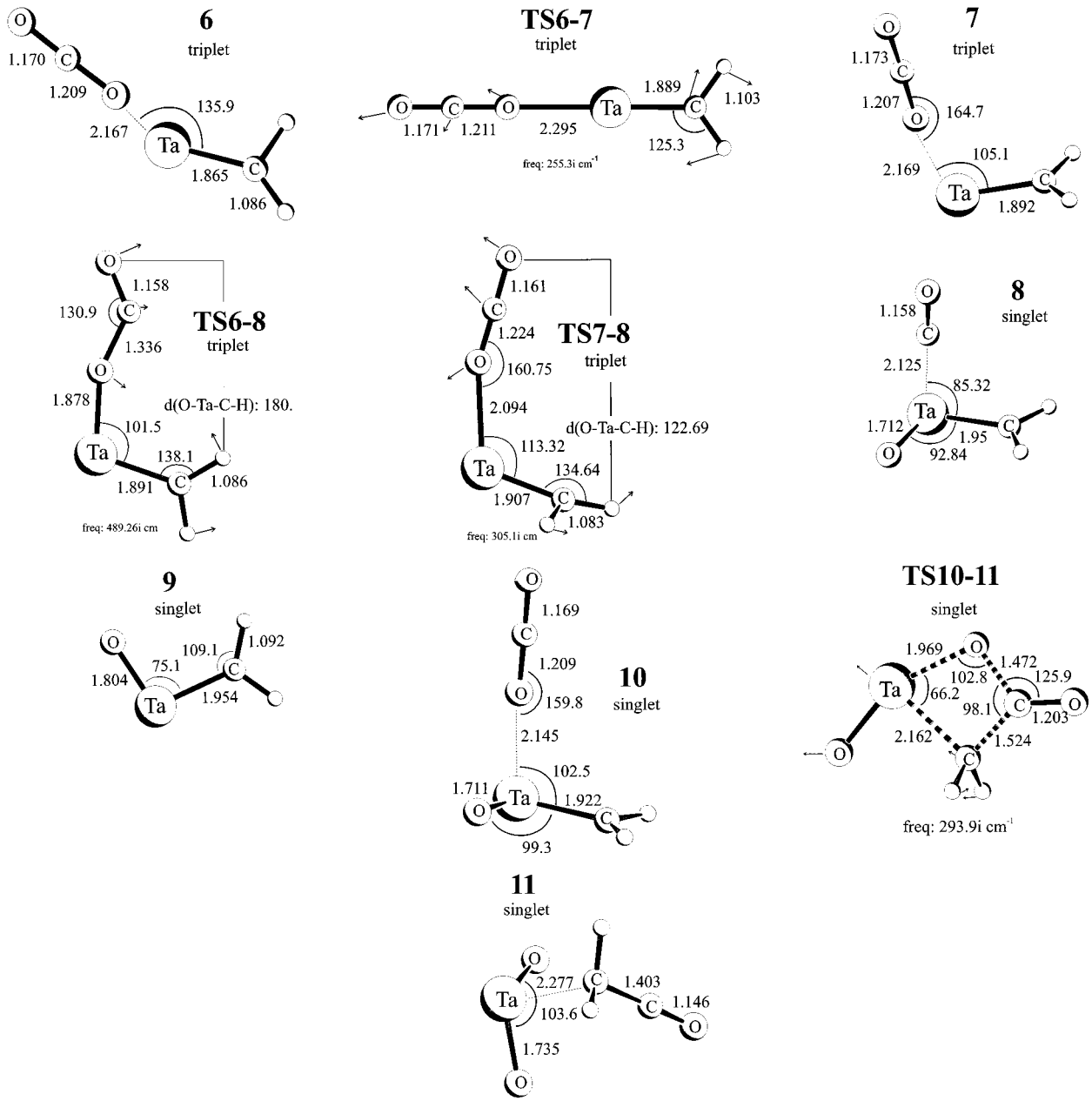

Figure 1. Geometries optimized at B3LYP and BS1: bond lengths in Å, bond angles in degrees. For the transition structures, the magnitudes of the imaginary frequencies and the corresponding transition vectors are also shown.

donor. The observed products were a vinylidene ($C{=}CH_2$) and a Ta−O moiety.[22]

Results and Discussion

Figure 1 displays the geometrical features of all relevant species discussed in the present study, while Table 2 summarizes the computed energies. Only the geometries of the electronic ground states are given. Since the structures of **1**−**5** have been discussed previously,[8] they are not repeated here. The relative energies are given with respect to the entrance channel of the entire reaction, i.e., $Ta^+ + CH_4 + 2CO_2$, which defines 0 kcal mol^{-1}. The additional molecules needed to balance the stoichiometry are usually not explicitly given. Figures 2−4 contain the calculated ground-state potential energy surfaces corresponding to the three individual steps of the process $Ta^+ + CH_4 + 2CO_2 \rightarrow TaO_2^+ + C_2H_2O + CO + H_2$ as described above.

We commence our discussion with a very brief summary of our recent results on the first phase of this reaction, the insertion of the ground-state Ta^+ cation into a C−H bond, summarized in Figure 2. For a more detailed exposition, the reader is asked to consult our previous study.[8] The insertion reaction proceeds via the η^2 Ta^+−CH_4 complex **1** and is characterized by a fairly small activation barrier (8.9 kcal mol^{-1} for **TS1**−**2** with respect to **1**) to generate the cationic H−Ta^+−CH_3 complex **2**. This complex represents the global minimum along the reaction path for the C−H activation. A second α-hydrogen shift involving the transition state **TS2**−**3** (21.7 kcal mol^{-1} above **2**) leads to the intermediate dihydrido−methylene species **3**, followed by rearrangement to the dihydrogen complex of the cationic tantalum carbene, $(H_2)TaCH_2^+$ (**4**). The activation

(22) Proloux, G.; Bergman, R. G. *J. Am. Chem. Soc.* **1993**, *115*, 9802.

Table 2. Theoretical Thermochemistry (in kcal mol^{-1}) for the Species Relevant to the Reaction Ta (^{5}F) + CH_4 + $2CO_2$ → TaO_2^+ ($^1A_1$) + C_2H_2O + CO + H_2 with the Basis Set BS3

	BS3		
compd	ΔE_{rel}	ΔE_{ZPVE}	$\Delta G_{298\ K}$
Ta (^{5}F) + CH_4 + $2CO_2$	0.0[a]	0.0	0.0
Ta (^{3}F) + CH_4 + 2CO2	18.5	18.5	18.5
Ta (^{1}D) + CH_4 + $2CO_2$	45.2	45.2	45.2
1$_{quintet}$	−13.8	−13.5	−12.0
1$_{triplet}$	−10.3	−9.8	−9.4
1$_{singlet}$	12.9	13.3	13.1
TS1−2$_{triplet}$	8.2	3.4	−3.1
TS1−2$_{singlet}$	13.6	13.4	15.4
2$_{triplet}$	−31.4	−35.0	−43.4
2$_{singlet}$	−12.8	−16.8	−24.6
TS2−3$_{triplet}$	−10.9	−14.8	−21.7
TS2−3$_{singlet}$	−5.3	−12.1	−18.3
3$_{triplet}$	−8.2	−15.4	−24.9
3$_{singlet}$	−22.8	−30.0	−39.6
TS3−4$_{triplet}$	7.1	−2.9	−15.0
TS3−4$_{singlet}$	0.1	−7.2	−16.2
4$_{triplet}$	2.9	−7.5	−21.8
4$_{singlet}$	−0.9	−8.0	−19.3
$TaCH_2^+$ ($^3A_2$) + H_2 + $2CO_2$	9.4	−0.3	−14.2
$TaCH_2^+$ ($^1A'$) + H_2 + $2CO_2$	18.9	10.9	−3.9
6$_{singlet}$	−0.6	−7.6	−24.1
6$_{triplet}$	−13.7	−20.9	−37.6
TS6−7$_{singlet}$	1.7	−6.0	−20.1
TS6−7$_{triplet}$	−6.0	−13.9	−29.0
7$_{singlet}$	−7.6	−14.1	−28.5
7$_{triplet}$	−13.7	−20.4	−35.8
TS6−8$_{singlet}$	18.4	14.5	3.4
TS6−8$_{singlet}$	−9.8	−12.3	−23.3
TS7−8$_{singlet}$	−10.6	−13.5	−17.4
TS7−8$_{triplet}$	−27.5	−30.4	−35.4
8$_{singlet}$	−66.7	−73.3	−86.4
8$_{triplet}$	−49.9	−55.3	−70.3
$OTaCH_2$ (^{1}A) + CO + CO_2 + H_2	−15.3	−23.9	−48.8
$OTaCH_2$ (^{3}A″) + CO + CO_2 + H_2	8.9	1.4	−19.9
10$_{singlet}$	−55.2	−58.8	−75.4
10$_{triplet}$	−40.8	−45.3	−64.2
TS10−11$_{singlet}$	−5.3	−8.9	−22.1
TS10−11$_{triplet}$	−4.1	−8.0	−22.3
11$_{singlet}$	−72.4	−75.4	−91.2
11$_{triplet}$	−62.0	−66.3	−84.5
TaO_2^+ ($^1A_1$) + C_2H_2O + CO + H_2	4.6	−0.7	−60.5
TaO_2^+ ($^3B_2$) + C_2H_2O + CO + H_2	37.3	30.7	−48.6

[a] $\mathbf{E}_{tot}$ = −474.397 69.

barrier for the latter isomerization is connected with **TS3−4** and was located 23.4 kcal mol^{-1} above **3**. Finally, **4** loses molecular hydrogen, generating $TaCH_2^+$. The most eye-catching peculiarity of this C−H bond process activation is its nonadiabaticity. Along the lowest energy reaction path, three changes in spin multiplicity occur: The ground state of the tantalum cation is a quintet and, thus, the $Ta^+ + CH_4$ asymptote has $S = 2$. The lowest energy pathway involves a crossing from the quintet to the $S = 1$ triplet surface between **1** and **TS1−2**, between the triplet to the singlet surface ($S = 0$) toward **TS2−3**, and between the singlet back to the triplet surface between **TS3−4** and **4**.

We now turn to the target of the present investigation and begin with a discussion of the second part of the reaction coordinate, i.e., the carbon dioxide activation mediated by the tantalum carbene cation complex Ta=CH_2^+ (**5**). The corresponding potential energy surface is shown in Figure 3. Two almost isoenergetic structural minima, both belonging to C_s point group symmetry, were located for the encounter complex between Ta=CH_2^+ and CO_2. In the first one (**6**) all atoms are coplanar. However, the carbon dioxide approaches the cationic tantalum carbene not along the extension of the H_2C−Ta bond (which would conserve the C_{2v} symmetry of the carbene complex). In the more stable triplet species, the H_2C−Ta−OCO angle is 135.9°. The geometry of the other encounter complex (**7**) is also of C_s symmetry, but now the CO_2 attacks the CH_2Ta^+ in a plane perpendicular to the molecular plane of the $TaCH_2^+$ moiety. In both cases the triplet species are more stable than the singlets (13.5 and 7.3 kcal mol^{-1}, respectively) and are situated 37.6 and 35.8 kcal mol^{-1} below the overall entrance channel $Ta^+ + CH_4 + 2CO_2$ or, equivalently, 23.4 and 21.6 kcal mol^{-1}, respectively, below the preceding intermediates $TaCH_2^+ + CO_2$.

The saddle point **TS6−7** directly joining **6** and **7** is characterized by an imaginary frequency of 255.3i cm^{-1}, and the transition vector depicted in Figure 1 clearly identifies the expected movement of the carbon dioxide. The barrier height for the isomerization between **6** and **7** (i.e. the relative energy of **TS6−7**) amounts to 8.6 kcal mol^{-1} relative to **6**. Like the two minima, **TS6−7** is also a ground-state triplet; the corresponding singlet state is 8.9 kcal mol^{-1} less stable. **TS6−7** has a linear arrangement of the non-hydrogen atoms and adopts C_{2v} symmetry.

Proceeding along the reaction coordinate, the two encounter complexes between Ta=CH_2^+ and CO_2 are converted into **8**, which serves as the direct precursor for the loss of carbon monoxide and the transfer of one oxygen atom from the carbon dioxide to the tantalum carbene. Note that while **6** and **7** are triplet ground states, the favored electronic state of **8** is a singlet (16.1 kcal mol^{-1} below the $S = 1$ state) due to the formation of an additional covalent Ta−O bond. Thus, we again observe a change in multiplicity similar to the preceding methane activation part of this reaction. While the inclusion of spin−orbit interaction might well lead to a stabilization of the triplet state, this stabilization will probably be significantly smaller than 16 kcal mol^{-1}. The C_1-symmetric structure **8** contains a mostly electrostatic bond between carbon monoxide and the $[OTa{=}CH_2]^+$ unit (r_{Ta-CO} = 2.125 Å). This intermediate **8** is computed to be very stable and lies 86.4 kcal mol^{-1} below the entrance channel. It is therefore by far the most stable species in this CO_2 activation branch of the overall reaction.

6 and **7** are connected with **8** by the transition structures **TS6−8** and **TS7−8**, respectively. The activation barrier associated with **TS6−8** amounts to 14.3 kcal mol^{-1} relative to **6**, while the barrier connected with the transition from **7** to **8** is extremely small: only 0.4 kcal mol^{-1} with respect to **7**. In both cases, the ground states of the saddle points are located on the triplet surface; the corresponding singlet species are found to be 26.7 (**TS6−8**) and 18.0 (**TS7−8**) kcal mol^{-1} less stable. Thus, the switch from the triplet to the singlet surface will occur between the saddle points and **8**.

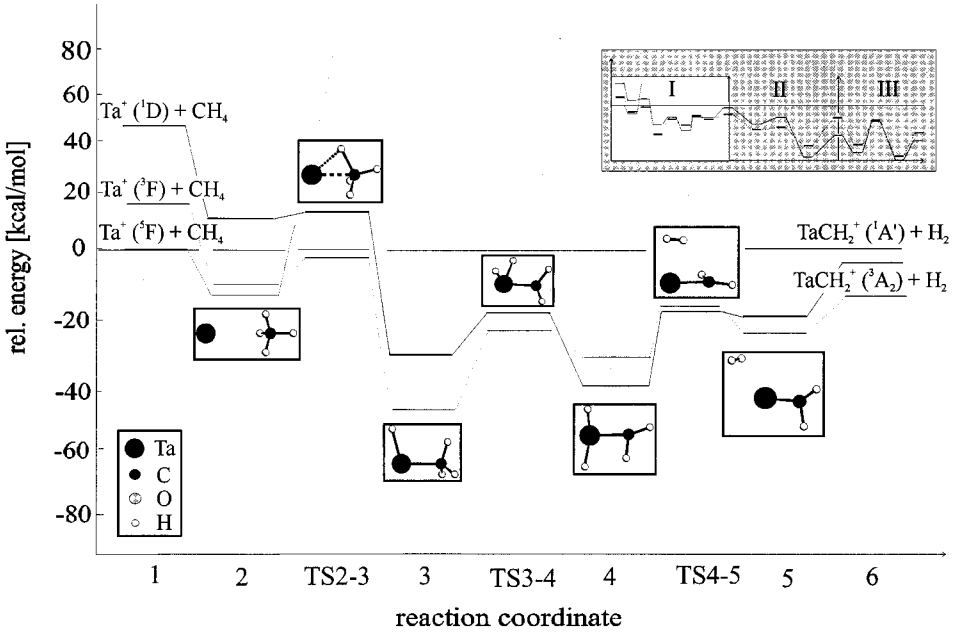

Figure 2. Computed ΔG^{298} surface of the C−H bond activation.

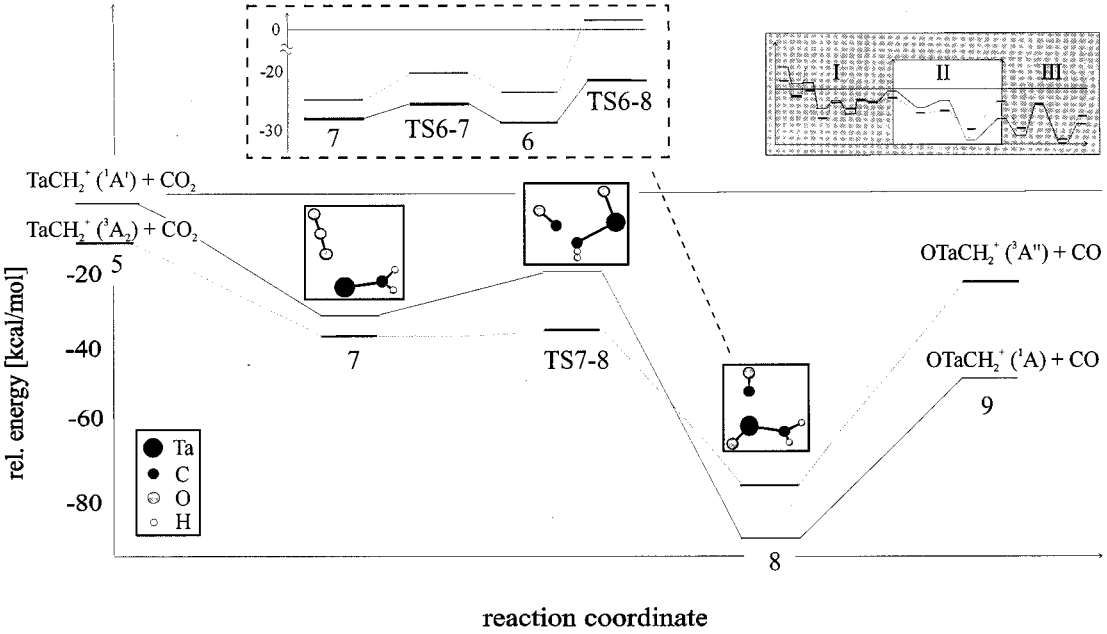

Figure 3. Computed ΔG^{298} surface of the first CO_2 activation.

TS6−8 and **TS7−8** are characterized by imaginary frequencies of 489.3 and 305.1 cm^{-1}, respectively. Both saddle points appear to be very early on their respective reaction coordinates. In particular, **TS7−8** is very reactant-like. The Ta−O bond is only slightly shorter than in **7**. The breaking of the C−O bond, which accompanies the Ta−O bond formation, is hardly visible in the transition structure and is only indicated by the small elongation of this bond from 1.207 Å in **7** to 1.224 Å in **TS7−8**. These geometrical changes are more pronounced in the energetically less favored **TS6−8**. Calculation of the intrinsic reaction coordinates show that indeed both **TS6−8** and **TS7−8** directly connect the corresponding minima with **8**. Since no change of multiplicity is of course possible in these strictly non-spin−orbit-coupled calculations, we confirmed these transition structures through the intrinsic reaction coordinates for both possible cases, i.e.; the reaction occurs adiabatically on the triplet or the singlet potential energy surface. While the subsequent chemistry will not be affected from the actual path leading from one of the encounter complexes (i.e. **6** or **7**) via either **TS6−8** or **TS7−8** to the product **8**, it is safe to assume that due to the rather low activation energy for the isomerization between **6** and **7** (via **TS6−7**) and the extremely low activation barrier connected with **TS7−8** this alternative will be favored, despite the slightly larger stability of **6** compared to **7**. Therefore, for the sake of clarity, only this path (i.e. **5** → **7** → **8**) has been explicitly included on the reaction coordinate in Figure 3.

The fate of **8** is to lose the electrostatically bound CO molecule. The final complex of the second part of the reaction sequence is therefore a $[Ta,C,H_2,O]^+$ structure formed through loss of carbon monoxide from **8**. As alluded to above, the experimental results suggest that

only two out of the five possible structures for this complex are likely but a clear-cut distinction was not possible (**a**−**e**, Chart 1). To shed more light on the actual structure of this $[Ta,C,H_2,O]^+$ intermediate, we optimized all possible isomers. The total energy of the singlet species $OTaCH_2^+$ (**a**) calculated with basis set BS1 amounts to −110.480 72 hartrees. The stabilities of the other structures are with respect to this total energy and do not include any corrections due to ZPVE etc. The experimental data favored the oxo−carbene complex **a** and the cyclic species **c** as being the most likely structural candidates. Our calculations indicate that the singlet oxo-carbene complex **a** is indeed the isomer with the lowest total energy. The corresponding triplet lies 24.2 kcal mol^{-1} above the singlet. The ground state of the oxametallocycle **c** is a triplet but is 30.5 kcal mol^{-1} less stable than the singlet state of **a** (and 7.9 kcal mol^{-1} more stable than the corresponding singlet). Since the loss of an OH radical was not observed in the experiments, the formation of the hydroxy−carbene complex **b** is unlikely. Nevertheless, the calculations indicate that this isomer lies energetically between the open $OTaCH_2^+$ (**a**) and the cyclic $OTaCH_2^+$ (**c**) species. Its singlet $S = 0$ state is the ground state, 16.4 kcal mol^{-1} less stable than the singlet $OTaCH_2^+$ species **a** and 11.7 kcal mol^{-1} below the corresponding triplet. The two other complexes, $Ta-OCH_2^+$ (**d**) and H_2-Ta^+-CO (**e**), are so much higher in energy that they can be safely ruled out as viable product complexes. The relative energies of the triplet and singlet Ta^+−formaldehyde complexes amount to 42.9 and 60.3 kcal mol^{-1}, respectively. The H_2-Ta^+-CO complexes are even more disfavored. The energy gap to singlet **a** amounts to 66.5 and 82.3 kcal mol^{-1} for the singlet and triplet, respectively. Thus, we assign the structure of **a** to the $[Ta,C,H_2,O]^+$ species **9**.

The energy of **9** ($S = 0$) was recomputed with the larger BS2. At this level, including contributions from ZPVE, thermal corrections, and entropy, the Gibbs free energy of **9** + CO + CO_2 + H_2, which defines the exit channel of the carbon dioxide activation by tantalum carbene, lies 48.8 kcal mol^{-1} below the entrance channel of the overall reaction, i.e., $Ta^+ + CH_4 + 2\ CO_2$.

To summarize, the computational results of this part of the reaction sequence are in accord with the experimental data and provide the desired insight into the mechanism at the molecular level. The reaction is significantly exothermic, and the computationally predicted reaction mechanism leads to the expected $OTaCH_2^+$ species. It is this ion which in the subsequent and final step reacts further with a second carbon dioxide.

The final and crucial part of the reaction sequence is the C−C linking process between the methylene group of the $OTaCH_2^+$ ion and a second carbon dioxide, thus generating the C_2 compound $[C_2,H_2,O]$ and cationic tantalum dioxide. Its potential energy surface is depicted in Figure 4. The reaction is initiated by the formation of an electrostatically bound encounter complex between the $OTaCH_2^+$ ion (**9**) and CO_2. This complex (**10**) where the carbon dioxide approaches the $OTaCH_2$ plane from above has, just as its precursor **9**, a singlet ground state and lies 26.6 kcal mol^{-1} lower in energy than separated **9** and CO_2 (or, equivalently, 75.4 kcal mol^{-1} below the overall entrance channel). The corresponding triplet is 11.2 kcal mol^{-1} less stable than the singlet species. Again, this energy separation is expected to be larger than the possible stabilization of the triplet due to spin−orbit interaction.

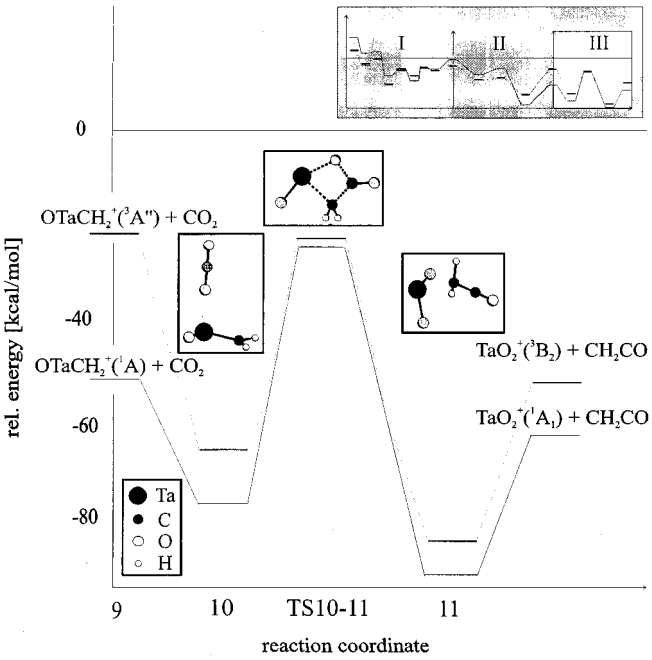

Figure 4. Computed ΔG^{298} surface of the C−C coupling process.

The next intermediate along the reaction coordinate is **11**, which serves as a product-like complex between cationic tantalum dioxide and ketene $H_2C{=}C{=}O$. The ground state of the C_1-symmetric structure **11** is also a singlet. It contains a mostly electrostatic bond between the positively charged tantalum dioxide and a neutral ketene molecule. **11** is the most stable species of the whole reaction sequence, located 91.2 kcal mol^{-1} below the entrance channel or 15.8 kcal mol^{-1} below **10**. The triplet of **11** is 6.7 kcal mol^{-1} less stable.

Transition structure **TS10**−**11**, which is of C_1 symmetry, adiabatically connects minima **10** and **11** on the singlet surface. It is characterized by an imaginary frequency of 293.9i cm^{-1}, and the transition vector describes the expected movements of the atoms (see Figure 1). Starting from **TS10**−**11** and following the intrinsic reaction coordinate confirmed the direct connection between this transition state and the two minima **10** and **11**. The theoretically computed barrier to this saddle point (**TS10**−**11**) is 53.3 kcal mol^{-1}, with respect to the minimum **10**. This is significant in terms of the thermodynamics of this reaction. It should be noted that in our calculations the singlet state of this saddle point is slightly less stable than the corresponding triplet ($\Delta\Delta G = 0.2$ kcal mol^{-1}). However, this energy difference is certainly far too small to allow for an unambiguous conclusion. In addition, the quantitative effect of spin−orbit interaction is not known and adds to the uncertainty of the energetic ordering for this saddle point. **TS10**−**11** is a four-membered-ring structure in which all existing bonds are lengthened. It is a typical example for a *concerted* metathesis reaction in which two bonds are broken (here the $Ta-CH_2$ and one

Table 3. Gibbs Free Energy for Two Possible Exit Channels in Both Spin Multiplicities, Singlet and Triplet, Calculated with Becke3LYP and Basis Set BS2

exit channel	ΔG (kcal mol^{-1})
$Ta{=}O^+ + CH_2CO$ singlet	−14.3
$Ta{=}O^+ + CH_2CO$ triplet	−29.6
$O{=}Ta{=}O^+ + CH_2CO$ singlet	−60.5
$O{=}Ta{=}O^+ + CH_2CO$ triplet	−48.9

C−O bond) and two new bonds are formed (here a Ta−O and a C−C bond) at the same time. No zwitterionic or radicaloid intermediates are involved in the present mechanism. In contrast, for the similar reaction observed by Proulx and Bergman in the condensed phase a two-step metathesis mechanism with a zwitterionic intermediate was suggested.[22]

This completes our detailed view on the reaction mechanism of the Ta^+-mediated C−C coupling reaction between CO_2 and CH_4. However, one needs to ask, why does the reaction proceed all the way until TaO_2^+ and ketene are formed instead of stopping after the activation of the first carbon dioxide molecule? One could imagine that **6** or **7** undergoes a metathesis reaction similar to that for **11**, which would lead to the generation of a ketene and $Ta{=}O^+$ rather than TaO_2^+. Table 3 shows the free Gibbs energies of this conceivable exit channel ($TaO^+ + H_2CCO$ [$+H_2 + CO_2$]) in comparison to the observed $TaO_2^+ + H_2CCO$ [$+H_2 + CO$] reaction with respect to the $Ta^+ + CH_4 + 2\ CO_2$ entrance channel (the molecules in brackets are needed to balance the stoichiometry of the reaction).

It is clear from the data listed in Table 3 that even from a thermochemical point of view a termination of the reaction after the first CO_2 activation is energetically not competitive. The corresponding products are computed to be only 29.6 kcal mol^{-1} more stable than the reactants if the triplet ground state of TaO^+ is formed. On the other hand, if the reaction proceeds as described above to finally yield singlet TaO_2^+ + ketene a significantly more pronounced exothermicity of 60.5 kcal mol^{-1} results. If we further assume that a barrier of similar height as **TS10**−**11** is connected with the hypothetical metathesis reaction leading to TaO^+ and ketene, a strong kinetic barrier is to be expected for this exit channel.

Conclusions

Density functional calculations employing the B3LYP hybrid functional combined with an adequate one-particle description were carried out in order to identify the mechanism of the experimentally observed Ta^+-mediated C−C coupling reaction between methane and carbon dioxide. The overall reaction proceeds through three steps with an overall computed exothermicity of −55.9 kcal mol^{-1}, in excellent agreement with the experimental number of −53 kcal mol^{-1}. In the first step a cationic tantalum carbene is formed, which acts as an activated form of CH_4. In the subsequent step, this carbene reacts with one molecule of CO_2 and generates a $[Ta,C,H_2,O]^+$ species accompanied by loss of CO. The structure of this intermediate was identified as $O{=}TaCH_2^+$, having a singlet ground state. In the last part of the reaction sequence, a second molecule of CO_2 reacts with $O{=}TaCH_2^+$. The final products are cationic TaO_2^+ and neutral ketene, $O{=}C{=}CH_2$, as the C−C-coupled species. This process proceeds as a concerted metathesis reaction in which $Ta{-}CH_2$ and one C−O bond are broken while simultaneously a Ta−O and a C−C bond are newly formed. While our computed reaction mechanism is in all aspects in agreement with the available experimental information, it provides additional insight into the various elementary steps of this reaction, which could not be obtained by experimental means.

Acknowledgment. This work was supported by the Deutsche Forschungsgemeinschaft, the Fonds der Chemischen Industrie, and the Gesellschaft von Freunden der TU Berlin. We thank the Konrad-Zuse Zentrum für Informationtechnik Berlin for providing a generous amount of computer time and excellent support (Dr. T. Steinke). Helpful discussions with Dr. M. C. Holthausen, Dr. R. H. Hertwig, Dipl.-Chem. T. K. Dargel, and Dr. R. Wesendrup are gratefully acknowledged.

OM971141L